J. Mol. Biol. (1989) **210**, 561–572

Insertion Sequence IS*10* Anti-sense Pairing Initiates by an Interaction Between the 5′ End of the Target RNA and a Loop in the Anti-sense RNA

J. D. Kittle[1]†, R. W. Simons[1,2], J. Lee[1] and N. Kleckner[1]‡

[1]*Department of Biochemistry and Molecular Biology Harvard University, Cambridge, MA 02138, U.S.A.*

[2]*Department of Microbiology University of California, Los Angles, CA 90024, U.S.A.*

(Received 18 January 1989, and in revised form 29 June 1989)

Transposition of insertion sequence IS*10* is regulated by an anti-sense RNA which inhibits transposase expression when IS*10* is present in multiple copies per cell. The anti-sense RNA (RNA-OUT) consists of a stem domain topped by a flexibly paired loop; the 5′ end of the target molecule, RNA-IN, is complementary to the top of the loop, and complementarity extends for 35 base-pairs down one side of RNA-OUT. We present here genetic evidence that anti-sense pairing, both *in vitro* and *in vivo*, initiates by interaction of the 5′ end of RNA-IN and the loop domain of RNA-OUT; other features of the reaction are discussed. In the context of this model, we discuss features of this anti-sense system which are important for its biological effectiveness, and suggest that IS*10* provides a convenient model for design of efficient artificial anti-sense RNA molecules.

1. Introduction

Insertion sequence IS*10* is part of the composite transposon Tn*10* (Fig. 1). IS*10* encodes a single transposase gene whose expression is regulated by DNA adenine methylation (Roberts *et al.*, 1985), by IHF protein (O. Huisman, P. Errada, L. Signon, D. Morisato & N. Kleckner, unpublished results; J. Sussman & R. Simons, unpublished results), and by an IS*10*-encoded anti-sense RNA (RNA-OUT). RNA-OUT pairs with the transposase mRNA (RNA-IN) over a 35 base-pair region of complementarity (Fig. 2), thereby preventing transposase gene translation (Simons & Kleckner, 1983). RNA-OUT probably inhibits translation directly by blocking binding of ribosomes, rather than by rendering the target RNA sensitive to double-stranded nucleases (C. Ma, C. Case & R. Simons, unpublished results).

IS*10* anti-sense control is also called "multi-copy inhibition" because it is important only when the element is present in more than a single copy per cell. Multi-copy inhibition was discovered because the activity of a single marked IS*10* or Tn*10* element in the chromosome is decreased ten to 30-fold upon introduction of a multi-copy plasmid containing IS*10* (Simons & Kleckner, 1983). More generally, as the number of IS*10* or Tn*10* copies per cell increases, the rate of transposition per copy decreases (J. Matsunaga, A. Toyofuku & R.W.S. unpublished results). The phenomenon of multi-copy inhibition results from two features of IS*10*. First, the effectiveness of anti-sense RNA control increases as the number of IS*10* copies, and hence the concentration of anti-sense RNA, increases. Second, IS*10* transposase is preferentially *cis* acting (Morisato *et al.*, 1983), so a decrease in the level of transposase made by a individual element results in a direct decrease in the level of transposition of that element.

Although a number of anti-sense RNA systems have not been described (for a review, see Simons & Kleckner, 1988), the pairing reaction mechanism has only been characterized in detail in one case, that of ColE1 (Tomizawa, 1984, 1985, 1987); *in vitro* pairing of P22 *sar* RNA and plasmid R1 *CopA* RNA has also been reported (Liao & McClure, 1988; Persson *et al.*, 1988). We consider below the mechanism of the IS*10* anti-sense RNA pairing reaction.

RNA-OUT forms a thermodynamically stable structure composed of a 21 base-pair "stem domain" topped by a "loop domain" whose most stable predicted structure includes two small duplex regions and a six-nucleotide loop (Fig. 3). The existence of such a structure is supported by

† Present address: Dept of Molecular Genetics, Ohio State University, Columbus, OH 43210, U.S.A.

‡ Author to whom correspondence should be addressed.

0022-2836/89/230561-12 $03.00/0

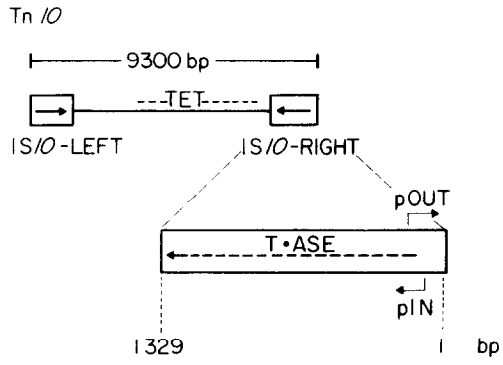

Figure 1. Tn*10* and IS*10*. P, Promoter; bp, base-pair(s). T-ASE, transposase.

the effects on RNA-OUT gel mobility of mutations which should alter base-pairing within the molecule and of agents that weaken or abolish RNA base-pairing (urea and glyoxal: Kittle, 1988). The precise conformation of the loop domain is not established. The 5′ end of RNA-IN is complementary to the top of the loop domain and complementarity extends down one entire side of the RNA-OUT stem.

We describe below the effects of mutations and other alterations on anti-sense pairing of IS*10*s RNA-IN and RNA-OUT *in vitro*. We find that pairing *in vitro* is affected only by mutations in the loop domain of RNA-OUT and the 5′ end of RNA-IN; changes in the RNA-OUT stem domain have no effect. Certain mutations alter the sequence specificity of the pairing reaction. We have also examined particular combinations of mutations for their effects on anti-sense control *in vivo*. A close correspondence between the effects of mutations *in vivo* and *in vitro* suggests that the same mechanism is used in both situations. On the basis of this analysis we propose that pairing initiates by an interaction between the 5′ end of RNA-IN and the loop domain of RNA-OUT; other features of the reaction are also considered.

Our analysis suggests that the role of the RNA-OUT loop domain is to present bases critical for pairing in a single-stranded form, while the RNA-OUT stem domain is not important for the rate of pairing. Experiments to be presented elsewhere show that the stem domain is responsible for RNA-OUT's unusual resistance to RNase attack *in vivo* (Case *et al.*, 1989). Initiation of pairing at the 5′ of RNA-IN is required for formation of fully paired duplexes, and may be important even for formation of a stable initial complex. We suggest that IS*10* is a convenient model for design of artificial anti-sense RNAs.

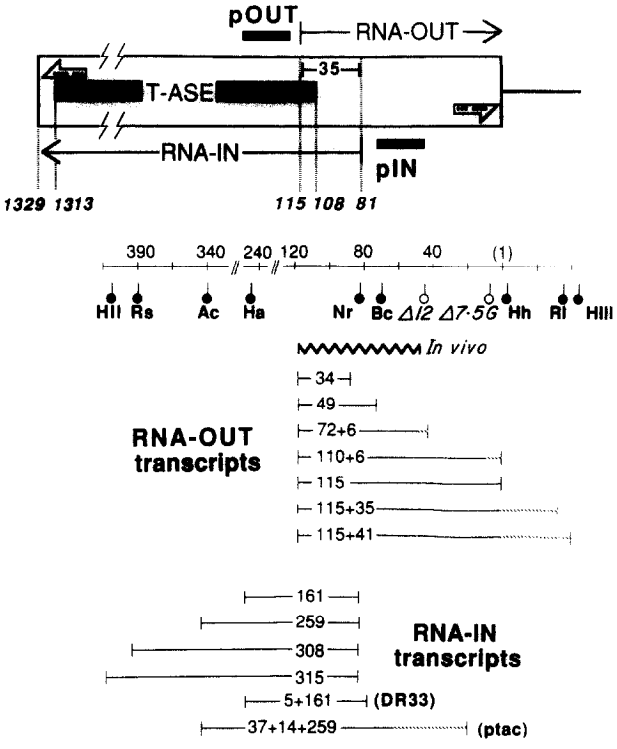

Figure 2. Structure of IS*10*. Transposase (T-ASE) gene (base-pairs (bp) 108 to 1319), RNA-IN and RNA-OUT transcription start points (bp 81 and 115, respectively), pIN and pOUT promoters, and nearly perfect terminal inverted repeats are shown. The 35 bp region of overlap between RNA-IN and RNA-OUT includes the start codon (bp 108 to 110) and the ribosome binding site of the transposase gene (see Fig. 3 and its legend). The extent of the predominant 69 base RNA-OUT species seen *in vivo* is indicated by a heavy jagged line just below the restriction site map (and Fig. 3). RNA species generated by *in vitro* transcription are also indicated: straight lines indicate sequences encoded by the corresponding wild-type IS*10* base-pairs on the restriction fragment map, while broken lines indicate non-IS*10* sequences present at certain 3′ or 5′ ends. Numbers indicate the number of nucleotides present in each transcript segment. *DR33* and *ptac* transcripts are described fully in Fig. 5. The endpoints of the Δ*12* and Δ*7·5G* deletions (open circles) are marked by a *Bam*HI linker, so templates ending at these *Bam*HI sites yield RNA-OUT transcripts containing an extra 6 bases of linker-encoded sequence. 115+35 and 115+41 transcripts contain 3′-terminal non-IS*10* sequences that flank IS*10* in the starting plasmids pNK190 and pNK200, respectively. Restriction enzyme cleavage sites indicated by filled circles were used to generate transcription template DNA fragments. HII, *Hin*cII; Rs, *Rsa*I; Ac, *Acc*I; Ha, *Hae*III; Nr, *Nru*I; Bc, *Bcl*I; Hh, *Hha*I; RI, *Eco*RI; HIII, *Hin*dIII.

2. Materials and Methods

(a) *Plasmids*

Plasmids carrying wild-type IS*10*-Right are pNK214 (Way & Kleckner, 1984), pRS449, which is a deletion between the *Acc*I and *Cla*I sites of pNK82 (Foster *et al.*, 1981), and pNK200, which is the IS*10*-Right *Hin*dIII fragment from λ171 (Kleckner, 1979) inserted at the *Hin*dIII site of pBR322. Isogenic mutant derivatives of pNK214 are pNK225 (*R5*), pNK956 (*insNB*), and pNK593 (*HH112*) described by Simons & Kleckner, (1983). Isogenic mutant derivatives of pRS449 are pRS440 (*mci1*), pRS441 (*mci10*), pRS443 (*mci15*), pRS514 (*mci30*), pRS519 (*mci60*) and pRS520 (*mci63*); isolation of these mutations will be described elsewhere (Case *et al.*, 1989). pNK1162 is an isogenic *DR33* derivative of pNK82 (Roberts *et al.*, 1985). Mutation *JL84* was constructed by

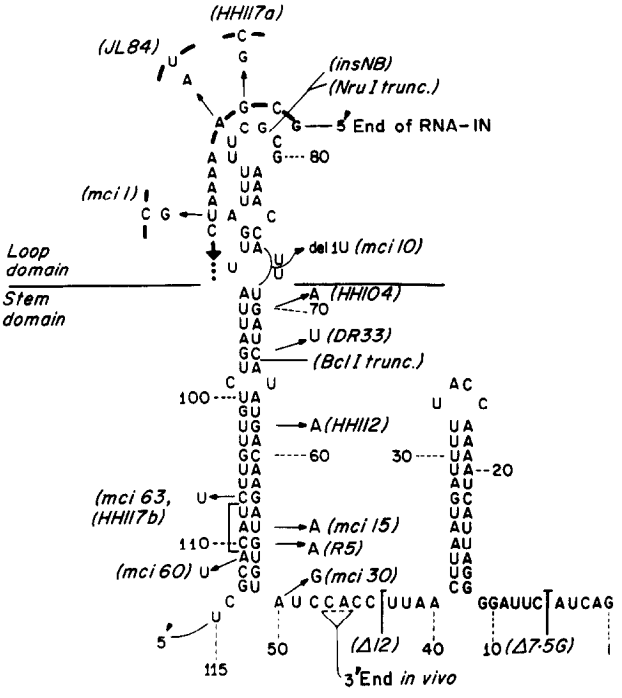

Figure 3. RNA-OUT and relevant mutations. The predominant RNA-OUT species observed *in vivo* begins at base-pair (bp) 115 of IS*10* and ends at bp 47. This RNA can be folded into an obvious secondary structure with an unambiguous stem domain topped by a less stably paired loop domain. The structure with the particular loop domain pairing shown here has a stability of $\Delta G = -22{\cdot}1$ kcal/mol (1 cal = 4·184 J) at 37 °C as calculated according to the Zucker–Stiegler (1981) program with the base-pairing free energy values given by Freier *et al.* (1986). For comparison, a structure with a completely unpaired loop domain differs from that shown by +4 kcal/mol. Additional IS*10* bases 3′ to the normal RNA-OUT terminus are shown because they are present on some of the *in vitro* transcripts analyzed. The trinucleotide complementary to the AUG start codon in the transposase gene (bp 108 to 110) is bracketed; bp 99 is especially important for ribosome binding as revealed by mutational analysis (C. Jain & N.K. unpublished results) and several limited Shine–Dalgarno homologies that include this base can be identified. Also indicated are a number of single base changes in RNA-OUT, the location of one insertion mutation (*insNB*, Fig. 6(c)), the 3′ ends of truncated RNA-OUT transcripts (*BclI trunc* and *NruI trunc*, sometimes referred to as Δ*Nru* and Δ*Bcl*), and the endpoints of 2 deletion mutations, Δ*12* and Δ*7·5G* (Fig. 2). For 3 mutations, the corresponding changes in RNA-IN are also indicated. Mutations *HH117b* and *mci63* have the same base change. Mutation *mci10* results in a deletion of 1 U in the indicated run of U residues.

a specially developed oligonucleotide mutagenesis procedure and is carried by pNK1537, a plasmid very similar to pRS449 (unpublished results). Other plasmids carrying mutant IS*10* elements have been described: pNK474 (Morisato *et al.*, 1983); pNK290 (*HH104*), pNK433 (*HH117*), pNK693 (Δ*7·5G*), and pNK691 (Δ*12*) (Simons & Kleckner, 1983).

(b) *Template fragments*

Restriction fragments generated by cleavages of CsCl-purified plasmid DNAs were separated by polyacrylamide gel electrophoresis. Bands were visualized by staining with ethidium bromide and illumination with long wavelength ultraviolet light. Fragments of interest were recovered from excised bands by electroelution.

Specific template fragments were as follows. Fig. 4: wild-type RNA-IN (161) and wild-type RNA-OUT (115) from *Hae*III–*Hha*I fragment of pRS449, wild-type RNA-IN (161) and *HH104* RNA-OUT (115 to 35) from *Hae*III–*Eco*RI fragment of pNK290. Table 1: for reactions in order from top to bottom of Table: *Hae*III–*Hha*I of pNK1162 for RNA-IN and *Hae*III–*Hha*I of pRS449 for RNA-OUT; *Acc*I–*Eco*RI of pNK474 for RNA-IN and *Hae*III–*Hha*I of pRS449 for RNA-OUT; *Rsa*I–*Hin*dIII of pNK200; *Acc*I–*Bam*HI of pNK693 and pNK691; *Hae*III–*Hha*I of pRS449; *Hae*III–*Bcl*I of pRS449; *Hae*III–*Nru*I of pRS449; *Hin*cII–*Eco*RI of pNK290; *Acc*I–*Eco*RI of pNK290; *Hae*III–*Eco*RI of pNK290. Table 2: for mutant by wild-type reactions, mutant RNA-OUT or RNA-IN species were from *Hae*III–*Hha*I fragments of mutant plasmids analogous to pRS449 (see section (a), above) and complementary RNA was the same as in the reference reaction; for reference reactions in section A and B, wild-type RNA-IN and *HH104* RNA-OUT were from the *Hae*III–*Eco*RI fragment of pNK290, with the single exception discussed in the legend; for reference reactions in section C, wild-type RNA-OUT and wild-type RNA-IN were from the *Rsa*I–*Hin*dIII fragment of pNK200. Fig. 7: heterologous reactions are described in Table 2 except *mci1* Δ*BclI* and *mci1* Δ*NruI* reactions, which involved RNA-OUT from the *Hae*III–*Bcl*I and *Hae*III–*Nru*I fragments, respectively, of pRS440, and both RNA-IN and a reference RNA-OUT from the *Hae*III–*Eco*RI fragment of pNK290. For homologous mutant reactions, mutant RNA-IN and RNA-OUT species were from the *Hae*III–*Hha*I fragment of mutant analogues of pRS449.

Plasmids for RNA-IN templates in Fig. 4 (left panel), Fig. 7, Table 1 (first 6 reactions of B) and Table 2C were grown in a Dam$^-$ strain (NK5772) to maximize pIN activity (Roberts *et al.*, 1985). When a template fragment was used to provide mutant RNA-OUT only (sections A and B of Table 2) plasmids were prepared in a Dam$^+$ strain (NK5640) to suppress pIN activity and thus prevent any significant synthesis of mutant RNA-IN transcripts.

(c) *Enzymes and chemicals*

Restriction enzymes, *Escherichia coli* RNA polymerase holoenzyme, DNA polymerase I Klenow fragment and phage T4 DNA ligase were all obtained from New England Biolabs; T_1 RNase was obtained from Boehringer–Mannheim Biochemicals. Other reagents included nucleoside triphosphates (Pharmacia), [α-^{32}P]CTP (New England Nuclear), glyoxal (40% aqueous solution; Sigma) and heparin sulfate (Calbiochem).

(d) In vitro *transcription reactions*

E. coli RNA polymerase was incubated with purified restriction fragment templates in buffer for 15 min at 37 °C to allow formation of open complexes. Standard conditions were: 50 mM-Tris·HCl (pH 8·0), 10 mM-$MgCl_2$, 5% (v/v) glycerol, 1 mM-dithiothreitol, 50 mM-RNA polymerase, 5 to 15 mM of each template fragment(s). Transcription was then initiated by addition of ribonucleotide triphosphates (final concentrations: 200 μM-unlabeled

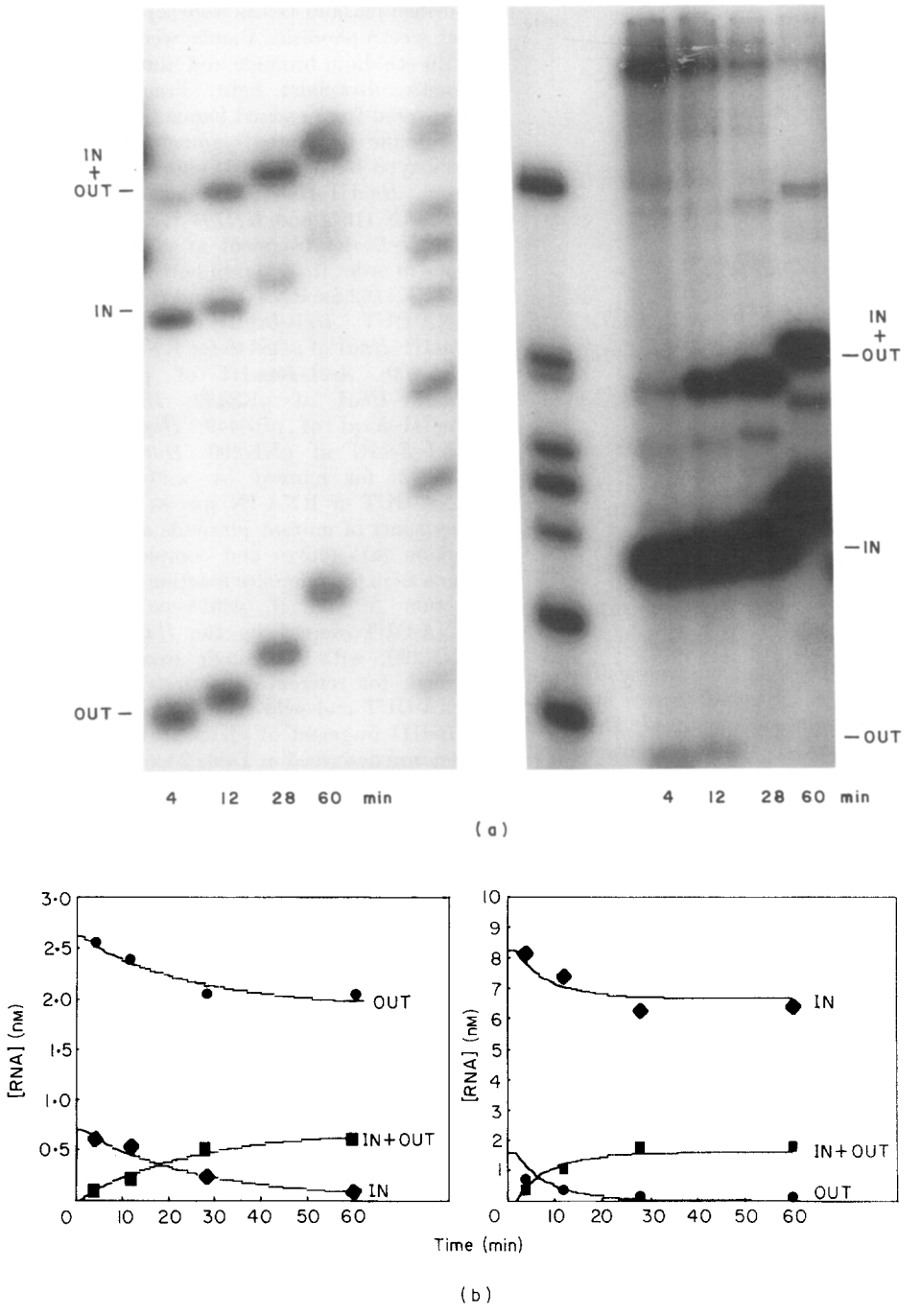

Figure 4. (a) The pairing assay. RNA-IN and RNA-OUT species were generated in the same *in vitro* transcription mixture. At the indicated times after the single round of transcription was initiated, samples were taken and loaded on a continuously electrophoresing non-denaturing polyacrylamide gel (Materials and Methods). In the left panel, RNA-OUT is present in excess over RNA-IN; in the right panel, RNA-IN is present in excess over RNA-OUT. The unpaired RNA-IN and RNA-OUT species and the species containing paired RNA-IN–RNA-OUT hybrids are indicated; minor bands are other transcripts routinely observed with these templates. Unpaired RNAs in the left panel are RNA-IN (161 nucleotides) and RNA-OUT (115); unpaired RNAs in the right panel are RNA-IN (161) and RNA-OUT (115+35). The latter RNA-OUT contains mutation *HH104*, which does not affect the rate of pairing (see the text) but increases the strength of pIN, thus making it possible to generate large amounts of RNA-IN. Template fragments are described in Materials and Methods. DNA size markers of 1621, 517, 506, 396, 298, 221, 220, 154 and 75 base-pairs were generated by *Hin*fI cleavage of pBR322 and end-labeled by standard methods (Maniatis *et al.*, 1982). Markers in left panel are 517 to 75; markers in right panel are 1621 to 154. (b) Determination of 2nd order pairing rate constants for the experiments in (a). Rate constants of 2·8 and $2{\cdot}9 \times 10^5$ M^{-1} s^{-1} were obtained for the reactions in the left and right panels, respectively. The radioactivity level in each band of interest was determined by excising and analyzing the gel slice for the amount of Čerenkov radiation. Background levels, determined by cutting and counting slices from regions of each lane that lacked discrete bands, were subtracted from each of the primary sample values. The concentration of each RNA species in the reaction mixture was then calculated using the Čerenkov data, the known base composition of each RNA species, the known specific activity of the radioactive label used for *in vitro* transcription, and the sample volume. Using these

ATP, GTP and UTP plus 30 μM-CTP labeled with (α-^{32}P), 30.000 μCi/μmol); heparin (100 μg/ml) was added along with rNTPs to prevent additional rounds of transcription initiation. Transcription was allowed to proceed at 37 °C; transcription was complete in less than 2 min.

(e) *Gel electrophoresis*

Gel electrophoresis was carried out with vertical 7% (w/v) polyacrylamide gels, 1·5 mm thick, using TBE buffer (Maniatis *et al.*, 1982). For analysis of pairing reaction samples, gels were pre-electrophoresed at 8 V/cm for 60 min and were kept running throughout the course of the reaction. Each sample was loaded as soon as it was taken, and immediately after each loading, the gel was run rapidly for 3 min (at 12 V/cm) and then returned to 4 V/cm until the next sample. When all samples were loaded, electrophoresis continued at 10 V/cm until completion.

(f) *Calculation of pairing rate constants*

Rate constants were determined for all reactions by fitting computer-generated model curves to the experimental data points. For each pairing reaction mixture, the following procedure was followed. First, initial concentrations of all relevant unpaired RNA species were determined as described for Fig. 4, legend. Second, a trial estimate of the rate constant for each pairing reaction in the mixture was selected. Third, theoretical curves for the disappearance of each unpaired RNA and appearance of each paired product species were generated from the initial unpaired RNA concentrations and the selected trial rate constants; the predicted concentrations of each reactant and product were calculated at successive 1-min time intervals after the start of the reaction. Fourth, the fit between this set of theoretical curves and the corresponding experimental data was determined by calculating the mean square differences between the observed and predicted data for all data points. Fifth, steps 3 and 4 were repeated, varying the trial constant systematically. The set of constants that best fit all of the data in a given experiment was defined as that which minimized the mean square difference between observed and predicted results. In all reactions, the fit was significantly enhanced by allowing the theoretical curve to be offset from the actual data by 1 to 2 min. A lag in the reaction of about this length of time is expected in view of the time required for transcription to be completed; the length of the lag did not depend on the actual concentration of any of the RNAs in the mixture. The above approach assumes that all pairing reactions occurring in a given mixture are independent of one another. For reactions given in Table 2A and B, RNA-IN is in sufficient excess that competition between mutant and wild-type RNA-OUT species is not significant. For homologous mutant reactions in Fig. 7, only mutant RNA species are present in the reaction. For reactions in Table 2C, 4 different pairing reactions are occurring. However, of these reactions, 3 have also been measured independently: wild-type by wild-type (Table 1), mutant by mutant (Fig. 7) and wild-type RNA-IN by mutant RNA-OUT (Table 2A). The same pairing rate constants are obtained for these 3 reactions in both types of assays, and thus we assume that all 4 reactions are occurring independent of one another in the complex mixture.

(g) *Bacterial and phage strains*

NK5640 (aka NN294) is *pro*$^-$ *endoI*$^-$ *r*$^-$ *m*$^-$ *su*$^+$. NK5772 is *dcm6 dam3 met*B1 *galK2 gal*T22 *lac*Y1 *tsx*78 *thi*1 *ton*A31 *mtl*1. NK6660 is *recA*56, pOX38 (Guyer *et al.*, 1981). NK7005 is *lacpro*ΔXIII Nal^r Rif^r *arg*$^-$ *recA*56 λ^r. NK5830 and NK6641 are described by Foster *et al.* (1981). All λ phages were derivatives of RP167, a *λimm*21 derivative with a unique *Eco*RI site (Maurer *et al.*, 1980) and are analogous in structure to phages described by Davis *et al.* (1985). λ1198 and λ1244 are, respectively, λ1197 and λ1193 lacking a *plac*UV5 promoter segment; λ1245 is an isogenic *JL84* derivative of λ1244.

(h) *Mating out assay for transposition*

Donor strains were grown from single colonies to 1 ml saturated cultures which were then diluted 20-fold, regrown to 2×10^8 /ml, and mixed with a 5-fold excess of recipient cells grown to 5×10^8 ml. The mating mixture was incubated with very gentle aeration for 60 min, vortexed, and plated on media to select for recipient cells that had received the Tet^r determinant from the Tn*10* element in the donor strain. For the experiment in Table 3, Nal^r Tet^r cells were selected. Control experiments revealed that a few such colonies arise by a spurious route. These spurious colonies could be identified because they release λ phages. All spurious colonies have been eliminated from the data presented in Table 3, either by direct analysis of exconjugant colonies or, for matings in which the spurious colonies represented a very small fraction of the total, by subtraction of their expected contribution. *In vivo* data for *mci1* and *HH117a* presented in Fig. 7 were carried out using derivatives of NK5830 as donors and NK6641 as recipients, and the counterselected marker was for streptomycin resistance.

3. Results

(a) *Wild-type RNA-IN and RNA-OUT pairing* in vitro *is a second-order reaction*

Formation *in vitro* of complexes between RNA-IN and RNA-OUT that are fully paired over the 35 base-pair region of complementarity occurs

concentration values and a computer modeling approach described in Materials and Methods, a rate constant was found that best described all 3 sets of data: disappearance of each unpaired species and appearance of the paired species. The experimental data points and the theoretical curves corresponding to the optimal rate constant are shown. The accuracy of both the experimental data and the rate constant optimization is quite good: experiments performed with similar templates on different days yielded rate constants varying by 10 to 25% (Table 2). In experiments like this one where the 2 interacting RNAs were synthesized in the same reaction mixture, the best 2nd order rate constant fit was obtained by assuming that the pairing reaction began 2 min after initiation of transcription; this delay presumably reflects the time required for synthesis of the 2 transcripts, as no further label is incorporated into RNA after this time. The same 2nd order rate constant is obtained if pairing is initiated by mixing 2 separate transcription reactions or purified RNA-IN and RNA-OUT molecules (Kittle, 1988).

Table 1

Effects of changes at 5′ or 3′ ends of RNA-IN or RNA-OUT on the rate of pairing in vitro

RNA-IN genotype	RNA-IN Length	×	RNA-OUT Genotype	RNA-OUT Length	Pairing rate constant ($\times 10^5$ M^{-1} s^{-1})
A. *Extension at 5′ end of RNA-IN*					
DR33	6+61	×	WT	115	0·6
ptac	37+14+259	×	WT	115	<0·15
B. *Variations at 3′ ends of RNA-IN and RNA-OUT*					
WT	308	×	WT	115+41	2·5
WT	259	×	WT	110+6 (Δ7·5*G*)	3·4
WT	259	×	WT	72+6 (Δ*12*)	3·6
WT	161	×	WT	115	3·1, 2·5, 3·6‡
WT	161	×	WT	49 (Δ*BclI*)	2·5
WT	161	×	WT	34 †(Δ*NruI*)	2·7
WT	315	×	WT†	115+35	3·6
WT	259	×	WT†	115+35	2·7
WT	161	×	WT†	115+35	2·9

Pairing between RNA-IN and RNA-OUT species was examined as described for Fig. 4; RNA species are described in Figs 2 and 5; restriction fragment templates are described in Materials and Methods.

† WT, wild-type. These transcripts contain mutation *HH104* for reasons described in the legend to Fig. 4; this mutation does not alter the rate of pairing.

‡ Three independent determinations.

Table 2

Pairing between mutant and wild-type RNAs

Mutant RNA	Pairing rate ($\times 10^5$ M^{-1} s^{-1}) Mutant by wild-type (A)	Reference (B)	(A)/(B)
A. *RNA-OUT loop domain*			
insNB	<0·17	3·5	<0·05
HH117ab†	<0·18	3·5	<0·05
JL84	<0·17	3·4	<0·05
mci1	<0·15	3·0	<0·05
mci10	3·7	3·8	1·0
B. *RNA-OUT stem domain*			
mci30	3·2	3·1	1·0
R5	2·7	2·6	1·0
mci15	2·7	2·7	1·0
HH112	3·2	3·7	0·9
DR33	2·8	2·4	1·2
HH104	3·3	2·9	1·1
mci63	2·8	3·1	0·9
mci60	2·6	2·6	1·0
C. *RNA-IN*			
HH117ab†	<0·18	3·4	<0·05
JL84	0·49	2·7	0·18
mci1	2·9	3·0	1·0

Pairing between a mutant RNA-OUT and a wild-type RNA-IN (A and B) or between a mutant RNA-IN and a wild-type RNA-OUT (C) was examined as described for Fig. 4 except that reactions were internally referenced in that both the mutant reaction of interest (A) and a fully wild-type pairing reaction (B) were occurring in the same tube at the same time, with reactants and products distinguishable by their mobilities. For analysis of mutant RNA-OUTs other than *HH104* reaction mixtures contained mutant RNA-OUT (115 nucleotides), *HH104* (RNA-OUT (115+35), and an excess of wild-type RNA-IN. For analysis of *HH104* RNA-OUT itself, the reaction mixture contained *HH104* RNA-OUT (115+35), wild-type RNA-OUT (115) and an excess of wild-type RNA-IN (161). For analysis of mutant RNA-INs, reaction mixtures contained mutant RNA-IN (161), wild-type RNA-IN (308) and an excess of wild-type RNA-OUT (115+41). Pairing reaction rates that satisfactorily described the disappearance of all 3 unpaired species and appearance of both paired species were determined as described in the legend to Fig. 4(b) and Materials and Methods.

† *HH117ab* is a double mutant (Fig. 3). We assume that the pairing defects of *HH117ab* RNA-OUT and RNA-IN are due to the *HH117a* mutation at bp83, since the *HH117b* mutation is identical with mutation *mci63*, which has no effect on pairing when present in RNA-OUT.

Table 3
Effects of JL84 *on multi-copy inhibition*

λ::Tn*10* Prophage	RNA-OUT plasmid:	Transposition frequency ΔIS*10* (A)	Wild-type (B)	*JL84* (C)	Level of M.C.I. (A)/(B)	(A)/(C)
Wild-type		132	5	60	26	2·2
JL84		20	8	3	2·5	6·3
Δ*tase*		<0·08	<0·08	<0·08		

Donor strains (NK6660 = *recA*56 pOX38) carried a single copy λ::Tn*10* prophage expressing RNA-IN and a multi-copy pBR-based plasmid expressing RNA-OUT; the levels of RNA-OUT from λ::Tn*10* prophage and RNA-IN from the plasmid are negligible. The recipient strain was NK7005 (= Δ*lacpro XIII* Nal^r Rif^r *arg*$^-$ λ^r). Single colonies of each donor strain were grown as small cultures and mixed with recipient cells to permit mating. Each mating mixture was plated on media selective for (Nal^r) recipient cells that had received the (Tet^r) Tn*10* transposon. Transposition frequency is the number of Tet^r Nal^r colonies obtained per ml of mating mixture plated; 100 colonies/ml represents an absolute rate of about 10^{-5} transposition events/Tn*10* element per cell generation. Each datum represents the average obtained from about 20 independent donor cultures, with 0·6 ml of each mating mixture plated. The level of multi-copy inhibition (M.C.I.) is the ratio of the transposition frequency obtained in the absence of any RNA-OUT (A) to the transposition frequency obtained in the presence of either (B) wild-type or (C) mutant RNA-OUTs. The basal level of TN*10 JL84* transposition is about that of wild-type Tn*10*, because the mutation decreases transcription initiation from pIN (J.D.K. unpublished results). Other mutations described in Fig. 7, *mci1* and *HH117a*, have no effect on wild-type Tn*10* transposition in single copy. λ::Tn*10* phages were: λ1244 (wild-type), λ1245 (*JL84*) and λ1198 (Δ*tase*). Plasmids were pRS534 (wild-type), pNK1537 (*JL84*) and pBR333 (Δ*IS10*). Δ*tase* is an in-frame deletion between the 2 *Nco*I sites in the transposase gene; it completely abolishes transposition activity.

with an apparent second-order rate constant of 3×10^5 M^{-1} s^{-1} at 37 °C (Fig. 4(a) and (b)). Such complexes were observed using uniformly labeled transcripts generated by *in vitro* transcription using DNA restriction fragment templates, purified *E. coli* RNA polymerase and (α-^{32}P)-labeled nucleoside triphosphates (Materials and Methods). When labeled RNA-IN and labeled RNA-OUT are allowed to interact, pairing is observed as the appearance in a non-denaturing polyacrylamide gel of a new RNA species and disappearance of the two starting RNAs (Fig. 4(a)); the new species is composed of equal parts RNA-IN and RNA-OUT (data not shown). The new species detected in such analysis corresponds to complexes between RNA-IN and RNA-OUT that are completely paired before they are loaded on the gel, as shown by a comparison of the level of product observed in the gel assay and that found to be resistant to rapid T_1 nuclease digestion at the same time point (Kittle, 1988). Determination of pairing rate constants from gel data is described in the legend to Figure 4b and Materials and Methods.

(b) *Effects of deletions or extension on pairing* in vitro

Variations at the 5′ end of RNA-IN disrupt the pairing reaction (Table 1). *DR33* RNA-IN carries an additional five nucleotides of IS*10* sequence at its 5′ end (Fig. 5) and pairs at 20% the wild-type rate. *ptac* RNA-IN bears an additional 14 IS*10* bases 5′ to the normal startpoint plus 37 bases of heterologous material (Fig. 5) and does not give any detectable pairing (<5% the wild-type level).

In contrast, pairing between RNA-IN and RNA-OUT is not sensitive to variations at the 3′ end of either RNA. RNA-IN transcripts of 161 to 315 nucleotides in length and RNA-OUT of 34 to 115 nucleotides in length, some of which also contain short 3′ tails, all pair at the same rate, ±20% (Table 1). It is noteworthy that the shortest RNA-OUT molecule, RNA-OUT Δ*NruI*, contains only the bases complementary to RNA-IN.

(c) *Effects of single base changes on pairing* in vitro

All of the mutations in RNA-OUT and RNA-IN shown in Figure 3 have been examined for their effects on pairing in *in vitro* reactions where one RNA is mutant and the other RNA is wild-type (Table 2). Four mutations in RNA-OUT severely reduce pairing with wild-type RNA-IN, and all four map to the upper portion of the loop domain. In contrast, none of the eight single base changes in the stem domain of RNA-OUT has any effect on the ability of (mutant) RNA-OUT to pair with wild-type RNA-IN; some of these mutations decrease and some increase the calculated and observed (Kittle, 1988) stability of the RNA-OUT stem. A ninth mutation, *mci10*, located at the base of the loop domain, also has no effect on pairing.

Three of the four mutations that affect RNA-OUT pairing map in the region of complementarity between RNA-IN and RNA-OUT and were examined for their effects on RNA-IN activity in pairing with wild-type RNA-OUT. *HH117a*, *JL84* and *mci1* change the third, fourth and ninth bases from the 5′ end of RNA-IN, respectively (Fig. 3). The first two mutations, those closest to the 5′ end of RNA-IN, affect pairing of mutant RNA-IN with wild-type RNA-OUT: *HH117a* reduces pairing to an undetectable level (<5%) and *JL84* reduces

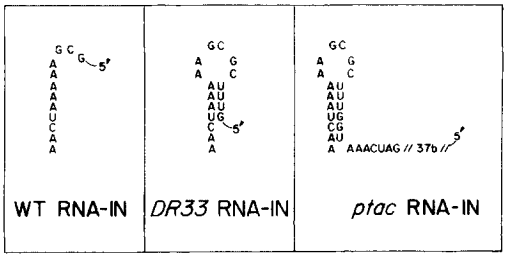

Figure 5. Primary sequence and potential secondary structures at the 5′ ends of wild-type, *DR33* and *ptac* RNA-IN molecules. The *DR33* mutation suppresses pIN and creates a new promoter just upstream that specifies a transcript 5 bases longer than wild-type (WT) RNA-IN (Roberts *et al.*, 1985; J.D.K. & R.W.S., unpublished results). *ptac* RNA-IN is the transcript specified by a template in which a segment bearing the heterologous *ptac* promoter has been inserted at the *Bcl*I site of IS*10* (Morisato *et al.*, 1983). The resulting transcript contains an additional 14 bases of IS*10* sequence upstream from the normal RNA-IN start point plus 37 bases of non-IS*10* material at its 5′ end.

pairing to 20% of the wild-type rate. The *mci1* mutation has no effect on pairing in this configuration.

(d) *Two mutations disrupt pairing by closing up the RNA-OUT loop domain*

The defects in *mci1* RNA-OUT and *insNB* RNA-OUT are a consequence of altered RNA-OUT secondary structure that sequesters loop domain bases important for pairing with RNA-IN. In both cases, inspection of the mutant RNA-OUT sequence suggests that intra-loop pairing should be stabilized by the mutation. *insNB* is an insertion of a symmetrical oligonucleotide linker that is predicted to allow formation of an extensive new secondary structure without altering any of the RNA-OUT bases in the region of complementarity (Fig. 6(c)). *mci1* creates a G·C pair which is predicted to stabilize strongly pairing within the loop domain (Fig. 6(b)); gel mobility assays under partially denaturing conditions confirm that *mci1* RNA-OUT is thermodynamically more stable than wild-type RNA-OUT (Kittle, 1988). The defect in *mci1* RNA-OUT is also not due to disruption of base-pairing between RNA-IN and RNA-OUT, since *mci1* RNA-IN pairs normally with wild-type RNA-OUT and, even more strikingly, *mci1* RNA-OUT is defective for pairing even with the completely homologous *mci1* RNA-IN (Fig. 7).

Direct evidence for this interpretation of the *mci1* defect is provided by the observation that the pairing defect of *mci1* RNA-OUT is fully alleviated by a 3′ truncation that removes all of the potential intra-loop secondary structure but not the mutant base itself (*mci1* Δ*Nru*). Furthermore, the defect is partially alleviated by an analogous truncation that removes only a portion of the intra-loop secondary structure, *mci1* Δ*BclI* (Figs 6(b) and 7); since this deletion reduces the stability of intra-stem pairing, it presumably reduces the equilibrium proportion of RNA-OUT molecules which exist in this (inhibitory) closed structure.

(e) *Mutations that alter the sequence specificity of the pairing reaction*

Mutation *HH117a*, at the third base of RNA-IN and the complementary base of the RNA-OUT loop, cleanly alters the sequence specificity of the anti-sense pairing reaction, thus implicating formation of this base-pair in a critical step of the reaction. *HH117ab* RNA-IN and *HH117ab* RNA-OUT each fail to pair with the complementary wild-type RNA but pair efficiently with one another, in fact at about twice the wild-type rate (Fig. 7). These effects are presumably due only to the *HH117a* mutation (see the legend to Table 2).

Mutation *JL84* has more complex effects, decreasing the two heterologous reactions to different extents and reducing, but not eliminating, pairing in the homologous mutant interaction (Fig. 7). This mutation has also altered the specificity of the reaction, though not as cleanly as mutation *HH117a*. The precise basis for the complex pattern of *JL84* phenotypes is not clear. The severe defect in pairing of *JL84* RNA-OUT with wild-type RNA-IN as compared with the other heterologous combination may reflect the presence of two large (purine) nucleotides at the mismatched position in the unfavorable case as compared with the two small (pyrimidine) nucleotides in the favorable case. The comparable pairing rates of the favorable heterologous and homologous mutant combinations may indicate that Watson–Crick hydrogen bonding at this position is not the most significant factor; for example, precise details of structure could be relevant.

(f) *Mutational effects* in vivo *correspond closely to* in vitro *effects*

Mutations *mci1* and *JL84* and a new isolate of mutation *HH117a* lacking the *HH117b* mutation were also analyzed in both heterologous and homologous mutant configurations for their effects on Tn*10* anti-sense control. *In vivo* analysis was carried out in strains where the target RNA-IN transcript was specified by a single copy Tn*10* element inserted in the *E. coli* chromosome and the anti-sense RNA-OUT species was provided by an appropriate multi-copy plasmid. The effects of anti-sense control on transposase expression from the target RNA were assessed by measuring changes in the frequency of transposition of the single copy Tn*10* element, which is known to vary directly with the level of transposase (Morisato *et al.*, 1983). The effectiveness of anti-sense control for any particular combination of RNA-IN and RNA-OUT is expressed as the parameter "level of multi-copy inhibition", which is the ratio of the transposition

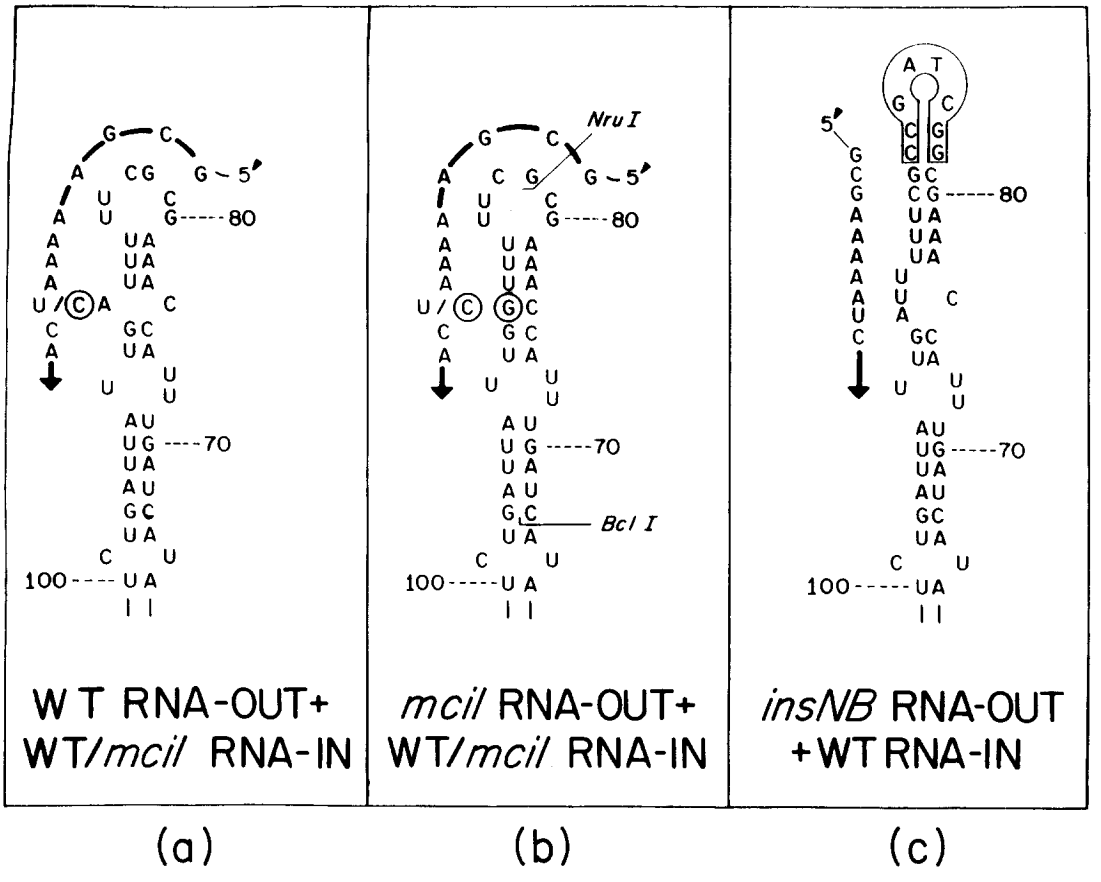

Figure 6. Consequences of *mci1* and *insNB* mutations. Wild-type (WT) and *mci1* RNA-IN's are juxtaposed to the structure of (a) wild-type RNA-OUT from Fig. 3 or (b) *mci1* RNA-OUT; the *mci1* mutant bases are circled. 3′ Ends of RNA-OUT molecules generated by truncation at the *Nru*I and *Bcl*I sites are indicated in (b). (c) Wild-type RNA-IN is juxtaposed to the altered sequence and proposed secondary structure for *insNB* RNA-OUT; the 8 additional bases of the *insNB* insertion are boxed.

frequency in the absence of any RNA-OUT to the transposition frequency in the presence of the RNA-OUT in question. This *in vivo* analysis is not compromised by effects of the analyzed mutations on steady-state RNA-OUT levels; each of the mutant RNA-OUT species analyzed below is known to have normal or nearly normal, *in vivo* stabilities (Case *et al.*, 1989).

Essentially, each of the mutations had the same effects *in vivo* as *in vitro*. Mutation *mci1* abolished control when present in RNA-OUT, regardless of whether the target was the homologous mutant or wild-type RNA-IN, and had almost no effect when present in RNA-IN. Mutation *HH117a* shows the same altered specificity phenotype *in vivo* as *in vitro*, abolishing control in the two heterologous configurations and, remarkably, improving control in the homologous mutant case. And mutation *JL84* has weaker effects similar to those seen *in vitro:* a significant residual level of control in the homologous mutant situation, and a severe defect in pairing of *JL84* RNA-OUT with wild-type RNA-IN. Pairing of wild-type RNA-OUT with *JL84* RNA-IN appears to be more defective *in vivo* than *in vitro*, for reasons that are not understood.

The correlation between *in vitro* and *in vivo* alterations also extends to *insNB* RNA-OUT and *DR33* and *ptac* RNA-INs; all of these RNAs are defective in anti-sense control when present in combination with a wild-type complementary RNA (Simons & Kleckner, 1983; Davis *et al.*, 1985; Roberts, 1986).

Three additional mutations that alter bases very near the 5′ end of RNA-IN and the complementary bases of RNA-OUT have been isolated and analyzed *in vivo* (R.W.S. *et al.*, unpublished results). Mutations *mciS10* at bp 82 and *mciS2* at bp 85, which affect the second and fifth base-pairs of the RNA-IN–RNA-OUT hybrid, respectively, exhibit the same clean altered specificity phenotype as *HH117a*. A third mutation, *mciC1*, is a transition mutation at the same site as *JL84*, and has a similar phenotype.

The nine stem domain mutations which do not alter pairing *in vitro* do abolish anti-sense control *in vivo*, but do so by altering features of anti-sense control other than the pairing process *per se;* some of these mutations decrease RNA-OUT stability and others increase the level of plasmid-promoted RNA-IN to the point where it titrates all of the RNA-OUT (Case *et al.*, 1989).

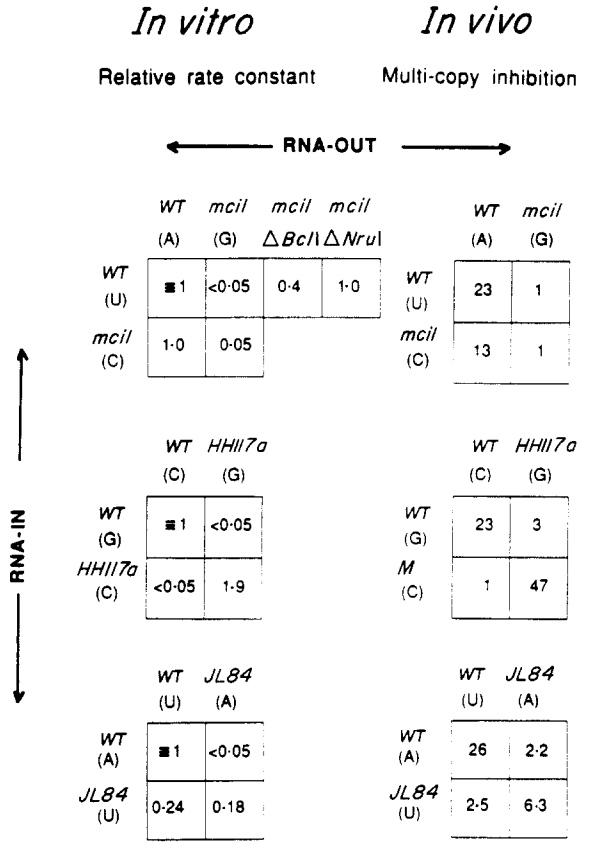

Figure 7. *In vitro* and *in vivo* analysis of the *mci1*, *HH117* and *JL84* mutations. Left panel: *in vitro* rate constants from Table 2 and analogous experiments. Right panel: level of multi-copy inhibition from Table 3 (*JL84*) and analogous experiments. The base present at the position of the mutation in question in each RNA is indicated in parentheses. *mci1* Δ*BclI* and *mci1* Δ*NruI* are described in Fig. 6 and the text. All 4 values in each box were obtained in the same single experiment.

4. Discussion

(a) *A model for RNA/RNA pairing*

The mutational analysis presented above shows that the rate of pairing depends critically on the nature of the RNA-OUT loop domain and the 5′ end of RNA-IN. All of the mutations or alterations which map to these regions alter the rate of antisense pairing *in vitro*, except for *mci10*, which affects a base at the bottom of the loop domain outside the region of complementarity; conversely, all of the mutations known thus far to alter antisense pairing *in vitro* map in these regions. The importance of these regions is further emphasized by the identification of the additional altered specificity mutations analyzed thus far only *in vivo*. In contrast, mutations which stabilize, destabilize or delete the RNA-OUT stem domain have no effect on the rate of pairing *in vitro*. We interpret these results to mean that an interaction between the 5′ end of RNA-IN and complementary bases in the RNA-OUT loop domain is critical to formation of a stable complex between these two RNAs, and that the stem domain poses no barrier to the rate of stable complex formation.

We further propose that pairing is initiated by an interaction involving the three G·C base-pairs at the 5′ end of RNA-IN (Fig. 8). Initiation of pairing at this location is attractive for several reasons. First, these three G·C base-pairs are followed by six A·U pairs, and nucleation of RNA oligonucleotide pairing (i.e. formation of the 1st base-pair on the pathway to complete pairing) occurs preferentially at G·C pairs (Cantor & Schimmel, 1980). Second, the existing data require that the third of these base-pairs must be involved at a rate-limiting step in the reaction; the *HII117a* mutation *increases* the rate of pairing, and must therefore affect the rate-limiting step. Third, initiation at the 5′ end of RNA-IN makes possible formation of RNA–RNA duplex over more than about one helical turn. Extensive pairing requires intertwining of the two complementary strands (e.g. see Tomizawa, 1984) and when pairing initiates at the end of RNA-IN, intertwining can be achieved by rotation of the nascent duplex around RNA-OUT. The failure of *DR33* and *ptac* RNA-IN molecules to pair efficiently may be due in part to interference with this rotation by their 5′ extensions, which must rotate in and out of the RNA-OUT loop during propagation of pairing. (Alternatively, these RNAs may fail to pair because sequences critical for initiation are sequestered in intra-molecular structure (Fig. 5).)

The kinetic details of the pairing reaction are likely to be complex. In oligonucleotide pairing reactions, formation of two or three base-pairs is sufficient to determine the rate of complete pairing (Cantor & Schimmel, 1980; Porschke & Eigen, 1971; Craig *et al.*, 1971). However, IS*10* anti-sense pairing differs substantially from the relatively simple interaction of two short oligonucleotides. The RNA-OUT bases involved in the likely initial interaction are present in a loop that has the potential to have significant structure, disruption of which could create additional barriers to nucleation of pairing. More significantly, perhaps, the anti-sense pairing reaction involves not simple pairing but the substitution of intra-molecular pairing within RNA-OUT by the formation of the IN–OUT duplex. The transition from simple strand pairing to strand displacement could occur as early as the fifth base-pair. After this point, propagation of pairing does not result in any net decrease in free energy except when a mismatch in the RNA-OUT stem is replaced by a perfect IN–OUT pair. These considerations suggest that the rate of the pairing reaction might not be determined until after formation of a considerable number of IN–OUT pairs. The fact that mutations at the fourth and fifth base-pairs can still disrupt the pairing reaction suggests either that the overall rate of the reaction has not been determined at this stage of the reaction, or that the pairing reaction is still sensitive to some new barrier imposed by the presence of an unpaired base at these positions.

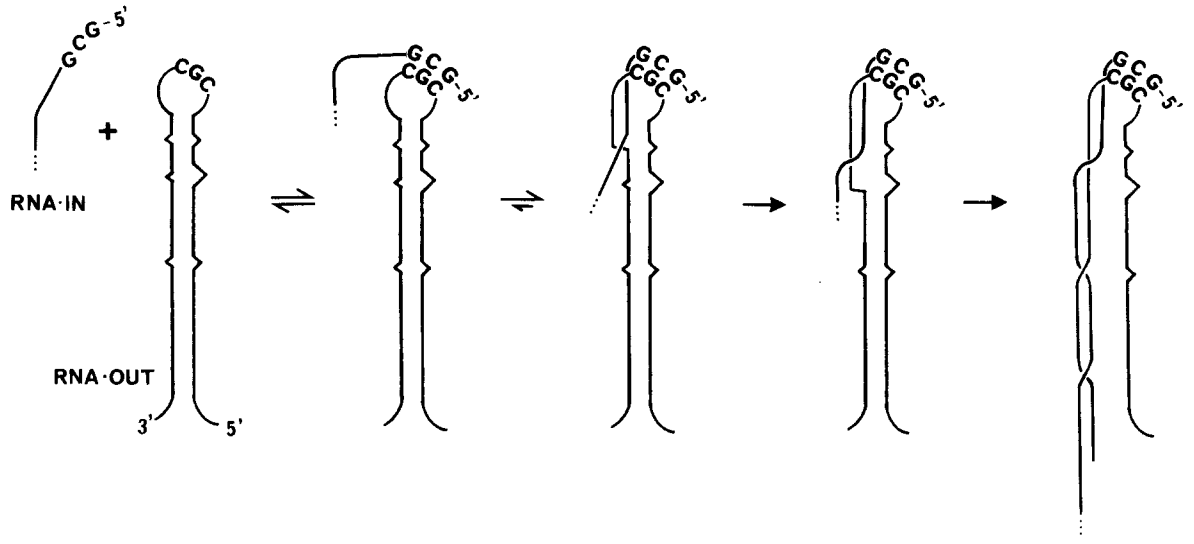

Figure 8. Proposed RNA-OUT–RNA-IN pairing reaction pathway. Initiation by interaction between the first 3 G or C bases at the 5′ end of RNA-IN and the corresponding bases in RNA-OUT is followed by extension of stable pairing through the loop domain and beyond through the stem domain of RNA-OUT.

The extent of pairing required for efficient IS*10* anti-sense control *in vivo* has not been fully investigated, and additional factors such as competition by 30 S ribosomal subunits could be relevant inside the cell.

(b) *Comparison with ColE1*

The IS*10* anti-sense reaction has not been analyzed in the same elegant detail as the ColE1 reaction; however, certain similarities are already apparent. At the most basic level, nucleating interactions involve single-stranded regions on both RNAs, and stable pairing initiates at a free RNA end (Tomizawa, 1984; and see above). However, the two reactions share other similar features which probably reflect the fact that formation of a small number of base-pairs is sufficient to determine the rate of the reaction and thus, as demonstrated explicitly for the ColE1 reaction, it is the kinetics rather than the thermodynamics of the interaction that are important (Tomizawa, 1985). Specifically, both reactions can be disrupted by single base changes in critical regions, with certain mutations changing the sequence specificity of the pairing reaction (Tomizawa & Itoh, 1981; Lacatena & Cesareni, 1981, 1983). In addition, the second-order rate constants for the two pairing reactions are rather similar to one another (Tomizawa, 1984, 1985) and to the forward association rates for complementary RNA oligonucleotide pairing (Cantor & Schimmel, 1980). The P22 *sar* and R1 *CopA* anti-sense reactions also share these same properties (Liao & McClure, 1988; Persson *et al.*, 1988).

(c) *Important structural features of IS10's anti-sense system*

Certain features of RNA-OUT and RNA-IN seem particularly important for efficient anti-sense control by the proposed mechanism. The loop domain of RNA-OUT presents bases critical for pairing in a single-stranded form. The stem domain of RNA-OUT has no role in the pairing reactions *per se*; however, experiments presented elsewhere (Case *et al.*, 1989) show that pairing within the stem domain, but not the loop domain, is crucial for RNA-OUT stability *in vivo*. Finally, as discussed above, initiation of RNA–RNA pairing at the 5′ end of RNA-IN makes possible formation of extensively paired duplexes.

(d) *IS10 as a model for artificial anti-sense RNAs*

IS*10* provides a convenient and relatively simple model for construction of artificial anti-sense RNAs, especially now that template DNAs of any desired sequence can be synthesized at will. To be effective, the anti-sense RNA should have a stem–loop structure analogous to that of RNA-OUT, with sequences homologous to one end of the target RNA located within the weakly paired loop domain. The stem region of this engineered RNA should be stable, but should not be perfectly base-paired, since increasing the extent of continuous pairing within the RNA-OUT stem by the *mci10* mutation renders the molecule sensitive to the double-strand-specific RNase III (Case *et al.*, 1989). For optimal effectiveness, the region of complementarity between the anti-sense and target RNAs should be long enough to make the paired species a substrate for RNase III, about two double-helical turns (Robertson, 1982); while normal IS*10* anti-sense control does not require RNase III cleavage (C. Case *et al.*, unpublished results), such cleavage could extend the efficiency of, or possibilities for, anti-sense control in artificial systems. Finally, the 5′ end of the target RNA should not contain any

secondary structure that would sequester bases involved in pairing.

We are grateful to Michael A. Davis and Denise Roberts for advice throughout this work and to many members of the Kleckner laboratory for comments on the manuscript. J.D.K. was supported in part by a National Science Foundation graduate student fellowship; R.W.S. was supported in part by post-doctoral fellowships from the Damon Runyan-Walter Winchell Cancer Fund and the Leukemia Society of America. This work was funded by research grants to N.K. from the National Science Foundation and the National Institutes of Health, and to R.W.S. from the National Institutes of Health and the American Cancer Society.

References

Cantor, C. R. & Schimmel, P. R. (1980). *Biophysical Chemistry*. Part III: *The Behavior of Biological Macromolecules*. W. H. Freeman and Co., San Francisco.

Case, C. C., Simons, E. L. & Simons, R. W. (1989). *EMBO J.*, in the press.

Craig, M. E., Crothers, D. M. & Doty, P. (1971). *J. Mol. Biol.* **62**, 383–401.

Davis, M. A., Simons, R. W. & Kleckner, N. (1985). *Cell.* **34**, 379–387.

Foster, T. J., Davis, M. A., Roberts, D. E., Takeshita, K. & Kleckner, N. (1981). *Cell.* **23**, 201–213.

Freier, S. M., Kierzek, R., Jaeger, J. A., Sugimoto, N., Caruthers, M. H., Neilson, T. & Turner, D. H. (1986). *Proc. Nat. Acad. Sci., U.S.A.* **83**, 9373–9377.

Guyer, M. S., Reed, R. R., Steitz, J. A. & Low, K. B. (1981). *Cold Spring Harbor Symp. Quant. Biol.* **45**, 135–140.

Kittle, J. D. (1988). Ph.D. thesis, Harvard University, Cambridge, MA.

Kleckner, N. (1979). *Cell.* **16**, 711–720.

Lacatena, R. M. & Cesareni, G. (1981). *Nature (London)*, **294**, 623–624.

Lacatena, R. M. & Cesareni, G. (1983). *J. Mol. Biol.* **170**, 635–650.

Liao, S.-M. & McClure, W. R. (1988). In *Molecular Biology of RNA. UCLA Symp. Mol. Cell. Biol. New Series*, vol. I. (Cech, T., ed.), **94**, Alan R. Liss, New York, in the press.

Maniatis, T., Fritsch, E. F. & Sambrook, J. (1982). Editors of *Molecular Cloning: A Laboratory Manual*, Cold Spring Harbor Laboratory Press, Cold Spring Harbor, NY.

Maurer, R., Meyer, B. & Ptashne, M. (1980). *J. Mol. Biol.* **139**, 147–161.

Morisato, D., Way, J. C., Kim, H.-J. & Kleckner, N. (1983). *Cell.* **32**, 799–807.

Persson, C., Wagner, E. G. H. & Nordstrom, K. (1988). *EMBO J.* **7**, 3279–3288.

Porschke, D. & Eigen, M. (1971). *J. Mol. Biol.* **62**, 361–381.

Roberts, D. (1986). Ph.D. thesis, Harvard University, Cambridge, MA.

Roberts, D., Hoopes, B. C., McClure, W. R. & Kleckner, N. (1985). *Cell.* **43**, 117–130.

Robertson, H. (1982). *Cell.* **30**, 669–672.

Simons, R. W. & Kleckner, N. (1983). *Cell.* **34**, 683–691.

Simons, R. W. & Kleckner, N. (1988). *Annu. Rev. Genet.* **22**, 567–600.

Tomizawa, J. (1984). *Cell.* **38**, 861–870.

Tomizawa, J. (1985). *Cell.* **40**, 527–535.

Tomizawa, J. (1987). In *Molecular Biology of RNA: New Perspectives* (Inouye, M. & Dudock, B. S., eds), pp. 249–259, Academic Press, New York.

Tomizawa, J. & Itoh, T. (1981). *Proc. Nat. Acad. Sci., U.S.A.* **78**, 6096–6100.

Way, J. C. & Kleckner, N. (1984). *Proc. Nat. Acad. Sci., U.S.A.* **81**, 3452–3456.

Zucker, M. & Stiegler, P. (1981). *Nucl. Acids Res.* **9**, 133–148.

Edited by N. Sternberg